REMARKS

Applicant respectfully requests reconsideration. Claims 1, 2, 22 and 34-59 were previously pending in this application. Claims 1, 36, and 38-42 have been amended. Support for the amendment can be found in the specification at least on page 8, lines 30-33; page 16, line 18-20; page 22, line 14 through page 23, line 19; and in Table 10 (pages 84-85). Claim 37 is canceled. No claims have been added. Claims 39 and 41 are currently withdrawn. As a result, claims 1, 2, 22, 34-36, 38, 40 and 42-59 are pending for examination with claims 1, 40 and 42 being independent claims.

No new matter has been added.

Objections to the Specification

The Examiner objected to the title as amended on May 22, 2009 because, according to the Examiner, the title does not disclose single domain antibodies specific for von Willebrand factor, the invention claimed in independent claim 1.

Applicant has amended the title to refer to single domain antibodies directed against von Willebrand factor, as suggested by the Examiner.

Accordingly, reconsideration and withdrawal of this objection is respectfully requested.

Rejections under 35 U.S.C. § 112, written description

The Examiner rejected claims 36-38, 40, 42, and 51-54 under 35 U.S.C. § 112, first paragraph, as allegedly failing to comply with the written description requirement. According to the Examiner, the claims contain subject matter which was not described in the specification in such a way as to reasonably convey to one skilled in the relevant art that the inventor, at the time the application was filed, had possession of the claimed invention for the reasons of record. Further, according to the Examiner, the rejected claims recite partial structure information for the antibody coupled with specific functional attributes for which, according to the Examiner, no correlation in the specification is provided.

Applicant respectfully disagrees, because the specification clearly conveys to the skilled person that Applicant had possession of the claimed polypeptides, polypeptide constructs, and compositions thereof, at the time of filing of the application, as is further explained below.

Applicant respectfully requests reconsideration, especially in light of the claim amendments presented herein.

Applicant has amended claims 36, 38, 40 and 42 to recite that the framework regions (FRs) of the homologous sequences of the single domain antibodies have a sequence identity of more than 85% with the framework regions of the parent sequences, or that the framework regions contain up to 10 amino acid substitutions, as compared to the framework regions of the parent sequence.

The scope of the claimed genus of polypeptides and polypeptide constructs and the claimed functionality is supported in the specification. The claims recite which specific regions (*i.e.,* the framework regions) of the single domain antibodies can be varied. As is well known in the art, a single domain antibody comprises CDR regions, which provide the single domain antibody its specific binding properties, and non-CDR regions (*i.e.,* the framework regions), which provide the structural characteristics of the single domain antibody. A person of ordinary skill in the art would appreciate that a limited number of amino acid substitutions (*e.g.,* up to 10 amino acids) in the framework regions will not interfere with the binding properties of the single domain antibody (See *e.g.,* pages 22 and 23 of the specification). A person of ordinary skill in the art would be able to rely on the specification or the state of the art to assess which amino acid changes can be introduced in the framework regions that do not interfere with the binding properties of the single domain antibody. For instance, references describing humanization of single domain antibodies provide which amino acid changes in the framework regions do not interfere with the binding properties of the single domain antibodies (See also pages 22 and 23 of the specification).

In addition, Applicant has provided a sufficient number of species to support the claimed genus of polypeptides or polypeptide constructs. Applicant has shown that humanization of single domain antibodies, which includes amino acid substitutions in the framework regions, does not interfere with binding properties of these single domain antibodies (See *e.g.,* pages 22 and 23 and Table 30 of the specification). In addition, which specific amino acid substitutions can be introduced in the framework region that do not interfere with the binding properties of single domain antibodies was known in the art. Applicant therefore has provided multiple sequences with amino acid substitutions in the framework regions that support the genus of

polypeptides or polypeptide constructs comprising single domain antibodies with amino acid changes in the framework region that can bind the target antigen.

The Examiner states that it is well known that the introduction of one or more mutations in the CDR regions of single domain antibodies would significantly alter the functionality (*i.e.*, binding properties) of the single domain antibody. Applicant submits that this concern by the Examiner has been addressed by amending the claims to recite that the amino acid changes in the single domain antibodies are located in the framework regions. As demonstrated above, amino acid changes in the framework region are not expected to interfere with the binding properties of the single domain antibodies.

Thus, at least for the reasons presented above, Applicant had possession of the claimed polypeptides, polypeptide constructs, and compositions thereof, at the time of filing of the application and Applicant therefore satisfies the written description requirement.

Accordingly, reconsideration and withdrawal of the rejection is respectfully requested.

Rejections under 35 U.S.C. § 112, enablement

The Examiner rejected claims 36-38, 40, 42 and 51-54 under 35 U.S.C. § 112, first paragraph, for alleged lack of enablement. According to the Examiner, the specification, while being enabled for antibodies comprising SEQ ID NO:5 or fragments of SEQ ID NO:5 that maintain the binding to the A1 domain of von Willebrand Factor (vWF), does not reasonably provide enablement for antibodies and fragments which comprise 70% identity to SEQ ID NO:5.

Applicant respectfully disagrees. Applicant submits that the specification provides enablement support for the claimed polypeptides, polypeptide constructs, and compositions thereof, as is further explained below. Applicant respectfully requests reconsideration, especially in light of the claim amendments presented herein.

Applicant has amended claims 36, 38, 40 and 42 to recite that the framework regions (FRs) of the homologous sequences of the single domain antibodies have a sequence identity of more than 85% with the framework regions of the parent sequences, or that the framework regions contain up to 10 amino acid substitutions, as compared to the framework regions of the parent sequence.

The test of enablement is not whether any experimentation is necessary, but whether, if experimentation is necessary, it is undue (MPEP §2164.01). Factors to be considered in

determining whether undue experimentation is required are summarized in *In re Wands* (858 F.2d 731, 8 USPQ 2nd 1400 Fed. Circ. 1988), and include (1) the quantization of experimentation necessary, (2) the amount of direction or guidance presented, (3) the presence or absence of working examples, (4) the nature of the invention, (5) the state of the prior art, (6) the relative skill of those in the art, (7) the predictability of the art, and (8) the breadth of the claims. Based on this amendment and on Applicant's showing herein as to the support in the specification and the state of the art, Applicant believes Applicant has met the burden of demonstrating that the claims meet the enablement requirement.

The specification teaches that amino acid substitutions in the framework regions do not interfere with the binding properties of the single domain antibodies. (See *e.g.,* pages 22-23 of the specification). In addition, the specification provides working examples of single domain antibodies with specific amino acid substitutions in the framework regions (See Table 30 and Example 63). Substituting amino acids in the framework region without altering the binding properties of the single domain antibodies was routine practice at the time of filing of the application. Single domain antibodies with framework regions with amino acid changes were known in the art, for instance in the humanization of single domain antibodies. The art provides which specific amino acid changes can be made in the framework region that do not interfere with the binding properties of the single domain antibodies (See for instance Vincke et al., "General strategy to humanize a camelid single-domain antibody and identification of a universal humanized nanobody scaffold, JBC 2009, 284: 3273, and references cited therein; Attached to this paper). A person of ordinary skill in the art can therefore rely on the specification and the routine art to practice the claimed invention without undue experimentation

The Examiner states that it is well known that the introduction of one or more mutations in the CDR regions of single domain antibodies would significantly alter the functionality (*i.e.,* binding properties) of the single domain antibody. In addition, the Examiner states that the working examples (which relate to changes in the framework region) are different in scope than the claims. Applicant submits that these concerns by the Examiner have been addressed by amending the claims to recite that the amino acid substitutions in the single domain antibodies are located in the framework regions. As demonstrated above, amino acid changes in the framework region are not expected to interfere with the binding properties of the single domain antibodies.

Thus, at least for the reasons presented above, a person of ordinary skill in the art can practice the claimed invention without undue experimentation thereby satisfying the enablement requirement.

Accordingly, reconsideration and withdrawal of the rejection is respectfully requested.

Rejections Under 35 U.S.C. § 103

The Examiner rejected claims 1, 2, 22, 34, 35, 43, 44-50, and 55 under 35 U.S.C. § 103(a) for allegedly being unpatentable over Nagano et al. (US Patent 5,916,805) in view of Ghahroudi et al. (FEBS Letters, 1997, 414:521-526). According to the Examiner, Nagano et al. discloses antibodies that bind vWF. However, according to the Examiner, Nagano et al. does not disclose heavy chain antibodies from *Camelidae*. Further, according to the Examiner, Ghahroudi et al. discloses heavy chain *Camelidae* antibodies, and it would have been obvious for a person of ordinary skill in the art to combine the teachings of Nagano et al. and Ghahroudi et al.

Applicant respectfully disagrees. The combination of Nagano et al. and Ghahroudi et al. does not render obvious the polypeptides and polypeptide constructs of the rejected claims, at least because the claimed polypeptides, polypeptide constructs, and compositions thereof, provide an unexpected result over the combination of Nagano et al. and Ghahroudi et al.

Applicant respectfully requests reconsideration of the claims as amended. Applicant has amended claim 1 and introduced the feature "wherein said single domain antibody is able to inhibit at least 50% of platelet aggregation at high shear (1600 s^{-1}) at a concentration of between 0.08 and 0.3 μg/ml.". Support for this feature can be found in the specification at least on page 16, lines 18-20 and in Table 10 (pages 84-85).

According to MPEP 2144.09, a *prima facie* case of obviousness based on structural similarity is rebuttable by proof that the claimed compounds possess unexpectedly advantageous or superior properties, citing In re Papesch, 315 F.2d 381, 137 USPQ 43 (CCPA 1963); and In re Wiechert, 370 F.2d 927, 152 USPQ 247 (CCPA 1967). Applicant submits that the claimed polypeptides and polypeptide constructs provide an unexpected result, consistent with MPEP 2144.09.

Applicant described platelet aggregation and summarized the results obtained at high shear rates found *in vivo* in Tables 10 and 11 (pages 84-85). Applicant discussed the unexpected nature of the results beginning at page 16, line 18:

> Surprisingly, monovalent VHH's perform very well in a platelet aggregation experiment under high shear: 50% inhibition of platelet aggregation was obtained at a concentration between 0.08 and 0.3 μg/ml. In comparison, the IgG vWF-specific antibody inhibiting the interaction with collagen, 82D6A3, inhibits 50% of platelet aggregation at approximately a twenty-fold higher concentration (Vanhoorelbeke K. *et al*, *Journal of Biological Chemistry*, 2003, 278: 37815-37821). These results were unexpected given that the IC50 values for the monovalent VHH's are up to 7 times fold worse in ELISA then the IC50 value of the IgG of 82D6A3.

These results show that monovalent vWF-binding VHHs were able to inhibit platelet aggregation to a greater extent than was expected based on the IC50 values of binding to vWF as assessed by ELISA. Specifically, platelet aggregation was inhibited using 20-fold less concentration of VHH than of monoclonal antibody 82D6A3. This was particularly surprising because the IC50 values of the VHH were 7 times worse than for the monoclonal antibody 82D6A3.

Nagano et al. (US 5,916,805) discloses monoclonal antibodies against vWF and evaluated these antibodies in a platelet aggregation experiment under high shear. The IC50 of these antibodies in a platelet aggregation experiment under high shear are 1.1 μg/ml on average (column 17 of US 5,916,805). The single domain antibodies of the rejected claims have an IC50 in a platelet aggregation experiment under high shear of at least 0.3 μg/ml or lower. Thus, the single domain antibodies of the rejected claims are much more potent in the ability to inhibit platelet aggregation under high shear than the monoclonal antibodies of Nagano et al. and therefore provide an unexpected result. This finding of increased potency is even more surprising because the monoclonal antibodies of Nagano et al. have two binding sites, while the single domain antibodies of the invention have only one binding site. Thus, the single domain antibodies of the invention provide an unexpected result compared to the antibodies of Nagano et al.

Ghahroudi et al. discloses heavy chain *Camelidae* antibodies. However, the teachings Ghahroudi et al. do not predict that *Camelidae* vWF antibodies based on the vWF monoclonal

antibodies of Nagano et al. will be more potent in the ability to inhibit platelet aggregation under high shear than the monoclonal vWF antibodies. Thus, the single domain antibodies of the rejected claims also provide an unexpected result over the combination of Nagano et al. and Ghahroudi et al.

The Examiner states that the data, as presented by Applicant, to support a finding of unexpected results, are not in commensurate in scope with the claims. Respectfully, Applicant submits that the data are in fact commensurate with the claims and support a finding of non-obviousness based at least on unexpected results for the claimed genus of polypeptides and polypeptide constructs. Applicant notes that the claims have been amended to limit the polypeptide and polypeptide constructs to single domain antibodies that inhibit platelet aggregation at a concentration of between 0.08 and 0.3 μg/ml. Applicant further notes that Table 10 provides several single domain antibodies and constructs that have the claimed functionality. Thus, the data support a finding of unexpected results for the claimed genus of polypeptides and polypeptide constructs and Applicant has provided "objective evidence of nonobviousness ... commensurate in scope with the claims which the evidence is offered to support." (See MPEP 716.02(d)).

In conclusion, the polypeptides and polypeptide constructs, and compositions thereof, of the claims provide unexpected results. Therefore, Applicant submits that the claimed invention is not obvious over the combination of Nagano et al. and Ghahroudi et al.

Accordingly, reconsideration and withdrawal of the rejection is respectfully requested.

The Examiner rejected claims 56-59 under 35 USC 103(a) as being unpatentable over Nagano et al. (US Patent 5,916,805) in view of Ghahroudi et al. (FEBS Letters, 1997, 414:521-526) as applied to claims 1, 2, 22, 34, 35, 43, 44-50, and 55 above, and further in view of Griffiths et al., (US Patent 5,670,132). According to the Examiner, the combination of Nagano et al. and Ghahroudi et al. discloses heavy chain *Camelidae* antibodies against vWF. However, according to the Examiner, the combination of Nagano et al. and Ghahroudi et al. does not disclose pegylated heavy chain *Camelidae* antibodies against vWF. Further, according to the Examiner, Griffiths et al. discloses pegylated antibodies and it would have been obvious according to a person of ordinary skill in the art to combine the teachings of Nagano et al. and Ghahroudi et al. with Griffiths at al.

Applicant respectfully traverses. The combination of Nagano et al., Ghahroudi et al. and Griffiths et al. does not render obvious the claimed polypeptides, polypeptide constructs and composition thereof at least because the polypeptides, polypeptide constructs, and compositions thereof provide an unexpected result over the combination of Nagano et al. and Ghahroudi et al. and Griffiths et al.

As demonstrated above, the claimed polypeptides, polypeptide constructs provide an unexpected result over the combination of Nagano et al. and Ghahroudi et al. The teachings of Griffiths et al. relate to the pegylation of antibodies in general and Griffiths et al. remains silent on the unexpected properties (*e.g.,* the potent ability to inhibit platelet aggregation) of the single domain antibodies of the claims. Thus, the claimed invention provides an unexpected result over the combination of Nagano et al. and Ghahroudi et al. and Griffiths et al.

Accordingly, reconsideration and withdrawal of the rejection is respectfully requested.

Double Patenting Rejection

The Examiner provisionally rejected claims 1, 2, 22, 34-38, 40, and 42-55 on the ground of nonstatutory obviousness-type double patenting as allegedly being unpatentable over claims 1,7, 16, 18, 19, 45, 56, and 66 of copending Application No. 10/534,349.

Applicant notes that the rejection is a provisional rejection. Applicant submits that a terminal disclaimer over U.S. Serial No. 10/534,349 may be provided, if appropriate, upon a determination of allowable subject matter.

The Examiner provisionally rejected claims 56-59 stand provisionally rejected on the ground of nonstatutory obviousness-type double patenting as being unpatentable over claims 1-7, 16, 18, 19, 45, 56, and 66 of copending Application No. 10/534,349 in view of Griffiths et al., US Patent 5,670, 132.

Applicant notes that the rejections is a provisional rejection. Applicant submits that a terminal disclaimer over U.S. Serial No. 10/534,349 may be provided, if appropriate, upon a determination of allowable subject matter.

CONCLUSION

A Notice of Allowance is respectfully requested. The Examiner is requested to call the undersigned at the telephone number listed below if this communication does not place the case in condition for allowance.

If this response is not considered timely filed and if a request for an extension of time is otherwise absent, Applicant hereby requests any necessary extension of time. If there is a fee occasioned by this response, including an extension fee, the Director is hereby authorized to charge any deficiency or credit any overpayment in the fees filed, asserted to be filed or which should have been filed herewith to our Deposit Account No. 23/2825, under Docket No. A0848.70010US00.

Dated: March 3, 2010

Respectfully submitted,

Electronic signature: /Erik J. Spek/
Erik J. Spek, Ph.D.
Registration No.: 61,065
WOLF, GREENFIELD & SACKS, P.C.
Federal Reserve Plaza
600 Atlantic Avenue
Boston, Massachusetts 02210-2206
617.646.8000

Attachment: Vincke et al. General Strategy to Humanize a Camelid Single- Domain Antibody and Identification of a Universal Humanized Nanobody Scaffold. *Journal of Biological Chemistry 2009*, 284: 3273-3284.

THE JOURNAL OF BIOLOGICAL CHEMISTRY VOL. 284, NO. 5, pp. 3273–3284, January 30, 2009

General Strategy to Humanize a Camelid Single-domain Antibody and Identification of a Universal Humanized Nanobody Scaffold*

Received for publication, September 5, 2008, and in revised form, October 31, 2008 Published, JBC Papers in Press, November 14, 2008, DOI 10.1074/jbc.M806889200

Cécile Vincke[‡§], Remy Loris[§¶], Dirk Saerens[‡§], Sergio Martinez-Rodriguez[§¶], Serge Muyldermans[‡§1], and Katja Conrath[‡§2]

From the [‡]Laboratory of Cellular and Molecular Immunology, [¶]Laboratorium voor Ultrastructuur, Vrije Universiteit Brussel, Pleinlaan 2, Brussels B-1050 and the [§]Department of Molecular and Cellular Interactions, Vlaams Instituut voor Biotechnologie, Brussels, Belgium

Nanobodies, single-domain antigen-binding fragments of camelid-specific heavy-chain only antibodies offer special advantages in therapy over classic antibody fragments because of their smaller size, robustness, and preference to target unique epitopes. A Nanobody differs from a human heavy chain variable domain in about ten amino acids spread all over its surface, four hallmark Nanobody-specific amino acids in the framework-2 region (positions 42, 49, 50, and 52), and a longer third antigen-binding loop (H3) folding over this area. For therapeutic applications the camelid-specific amino acid sequences in the framework have to be mutated to their human heavy chain variable domain equivalent, *i.e.* humanized. We performed this humanization exercise with Nanobodies of the subfamily that represents close to 80% of all dromedary-derived Nanobodies and investigated the effects on antigen affinity, solubility, expression yield, and stability. It is demonstrated that the humanization of Nanobody-specific residues outside framework-2 are neutral to the Nanobody properties. Surprisingly, the Glu-49 → Gly and Arg-50 → Leu humanization of hallmark amino acids generates a single domain that is more stable though probably less soluble. The other framework-2 substitutions, Phe-42 → Val and Gly/Ala-52 → Trp, are detrimental for antigen affinity, due to a repositioning of the H3 loop as shown by their crystal structures. These insights were used to identify a soluble, stable, well expressed universal humanized Nanobody scaffold that allows grafts of antigen-binding loops from other Nanobodies with transfer of the antigen specificity and affinity.

Minimizing the size of antigen-binding entities from a multidomain protein such as a monoclonal antibody to a single-chain variable fragment or even a single domain has been one of the primary goals of antibody engineering. For drug therapy, these smaller formats can be beneficial in various aspects such as immunogenicity, biodistribution, renal clearance, serum half-life, tissue penetration, and target retention. However, the minimal sized antibody fragments need to retain sufficiently high antigen specificity and affinity, be expressed in high yields, and should have a low tendency to aggregate so as to maintain maximal potency and reduce possible risks of immunogenicity. Moreover functionality in adverse environments such as high concentrations of denaturant or elevated temperatures, and a concomitant increased shelf-life are additional assets.

A significant proportion of the functional antibodies within species of the *Camelidae* are devoid of light chains. These immunoglobulins are referred to as heavy-chain antibodies (1), and their antigen-binding fragment is reduced to a single domain (referred to as VHH or Nanobody), with a molecular size of only ~15 kDa, which is smaller in comparison to single-chain variable fragment fragments (30 kDa), Fab fragments (60 kDa), and whole antibodies (150 kDa). All Nanobodies belong to the same sequence family, closely related to that of the human VH[3] of family III, although different subfamilies can be distinguished in dromedary based on the CDR2 length and the position of an additional cysteine in the CDR1 or the framework-2 (2). Because extra cysteines are rare in llama VHH sequences, they cannot be used as a subfamily hallmark and alternative subfamily divisions had to be proposed for llama VHHs (3, 4). Following immunization of a llama or dromedary, VHH genes can be easily cloned in a phagemid vector and antigen-specific VHHs can then be selected via phage display against virtually any antigen (5). Their small size, natural soluble behavior, and unique ability to target alternative epitopes make Nanobodies very attractive tools for tumor targeting, diagnostics, or even for *in vivo* therapy (6–10).

Analysis of the amino acid sequence of the Nanobodies obtained from immunized camelids revealed frequent substitutions in regions that are conserved in the VH domain of conventional antibodies. These Nanobody hallmark amino acids, located mainly in framework-2, are essential adaptations to avoid the association with the variable light chain domain (11). Most of these mutations are substitutions from a hydrophobic to a hydrophilic residue and are considered to increase the solubility of the isolated Nanobody (12, 13). In some cases, several of these residues at the "former VL-side" may also affect the

* The costs of publication of this article were defrayed in part by the payment of page charges. This article must therefore be hereby marked "*advertisement*" in accordance with 18 U.S.C. Section 1734 solely to indicate this fact.
The atomic coordinates and structure factors (codes 3DWT and 3EAK) have been deposited in the Protein Data Bank, Research Collaboratory for Structural Bioinformatics, Rutgers University, New Brunswick, NJ (http://www.rcsb.org/).
[1] To whom correspondence should be addressed. Tel.: 32-2-629-19-69; Fax: 32-2-629-19-81; E-mail: svmuylde@vub.ac.be.
[2] Present address: Galapagos NV, Generaal De Wittelaan L11 A3, B-2800 Mechelen, Belgium.

[3] The abbreviations used are: VH, heavy chain variable domain; LDA, ligation during amplification protocol; GdmCl, guanidinium chloride; r.m.s.d., root mean square deviation; CDR, complementarity determining region.

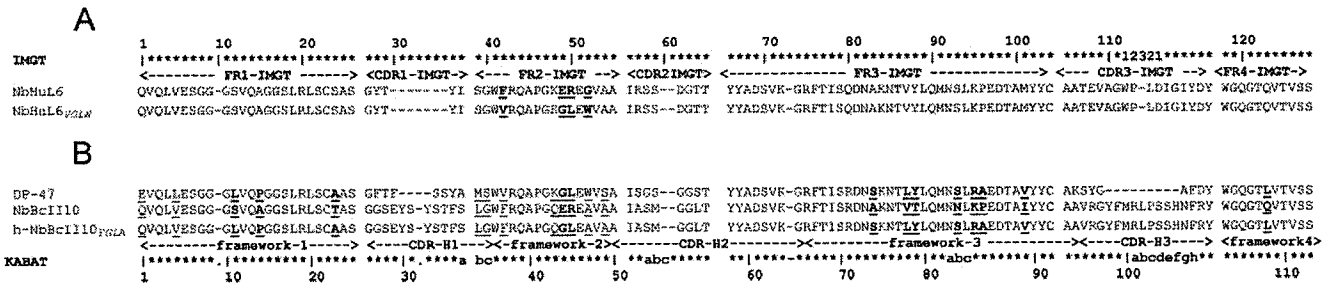

FIGURE 1. **Amino acid sequences.** *A*, NbHuL6 and NbHuL6$_{VGLW}$ with humanized residues in framework-2 (*italic*). *B*, human DP-47 reference framework sequence, NbBcII10 and h-NbBcII10$_{FGLA}$ with humanized framework. Differences in sequence from the reference human sequence are *underlined*. Framework residues that were mutated to their human counterpart are shown in *bold*.

antigen specificity of the Nanobody (13). These differences between VHH and VH conserved residues are Phe/Tyr-42 → Val, Glu-49 → Gly, Arg-50 → Leu, and Gly-52 → Trp (numbers refer to the International ImMunoGeneTics information system amino acid numbering (imgt.cines.fr)). Additionally, in ~10% of the Nanobodies, Trp-118 is substituted by an Arg (14). The Trp-118 → Arg substitution was proposed as an alternative option to further increase the solubility of single-domain antibody fragments (15).

Because mouse antibody fragments require a humanization step to be accepted as human therapeutics, it is likely that Nanobodies from camelid origin should also pass a humanization process. It is our objective in this work to assess the biochemical properties of several Nanobodies after such humanization effort. We investigated therefore the humanization of a couple of representative Nanobodies into more human-like antibody fragments and tested their retention of antigen-binding specificity. Two Nanobodies, members of subfamily-2, were chosen for this analysis: NbHuL6 (16) and NbBcII10 (17). Subfamily-2 is the most frequently occurring of the seven VHH subfamilies accounting for 75% of all isolated dromedary antigen-specific Nanobodies (2). We first focused on the framework-2 residues, because those mutations are expected to have the largest impact on expression, solubility, and antigen affinity of the isolated domain. We then analyzed the effect of the Trp-118 → Arg mutation on these antibody formats.

Subsequently, we substituted the remaining "non-human" residues in the framework and resurfaced NbBcII10 to obtain a humanized Nanobody scaffold (h-NbBcII10$_{FGLA}$) so as to exhibit the closest possible amino acid identity to a human VH (Fig. 1). It was previously demonstrated that the NbBcII10 accepts the CDR loops from a whole range of Nanobodies with transfer of the antigen specificity of the loop donor (18). Therefore, the CDR loops of two Nanobodies, NbHuL6 and NbHSA, were grafted on the resurfaced framework h-NbBcII10$_{FGLA}$, to assess whether this framework can indeed be used as a universal humanized Nanobody scaffold.

We determined and compared the antigen specificity, kinetic binding rate constants (k_{on}/k_{off}), the thermal (T_m), and conformational ($C_m/\Delta G^0$) stability parameters of multiple variants, humanized to different extents. To evaluate the impact of humanization on the scaffold architecture of Nanobodies, we solved the crystal structure of a partially humanized NbHul6 mutant (Phe-42, Gly-49, Leu-50, and Trp-52) in complex with its antigen and of the maximally humanized NbBcII10 (h-NbBcII10$_{FGLA}$). Based on this knowledge, a general strategy is proposed to generate a humanized version of any Nanobody with maximal retention of stability and antigen-binding characteristics. Finally, a universal humanized Nanobody scaffold was identified that accommodates antigen-binding loops from Nanobodies, even those from other subfamilies or species.

EXPERIMENTAL PROCEDURES

Site-directed Mutagenesis—Mutations were introduced by phosphorylated mutagenic oligonucleotides using the ligation during amplification protocol (LDA) (19). Multiple mutations were introduced simultaneously using multiple mutagenic primers, designed so as to add or eliminate a particular restriction enzyme site. The introduction of the different mutations was analyzed by restriction enzyme analysis and confirmed by DNA sequencing (ABI prism 3100 genetic analyzer, Applied Biosystems).

Expression and Purification of Nanobodies—The plasmid constructs were transformed into *Escherichia coli* WK6 cells. The expression in the periplasm and purification of recombinant His$_6$-tagged Nanobodies was performed as described previously (17). The purity of the proteins was evaluated by Coomassie-stained SDS-polyacrylamide gels. The protein concentration was determined spectrophotometrically at 280 nm using the computed extinction coefficient of each Nanobody, as calculated from their amino acid sequence (20).

Affinity Measurements—Different concentrations ranging from 500 nM to 7.8 nM of the NbHuL6, NbBcII10, and their respective variants were flown over a CM5 chip (Biacore) to which respectively human lysozyme (200 relative units) and BcII (800 relative units) had been coupled using the amine coupling chemistry (*N*-ethyl-*N*′-(dimethylaminopropyl)-carbodiimide/*N*-hydroxy succinimide) according to the manufacturer's descriptions. All measurements were performed at a flow rate of 30 μl/min in HBS buffer (10 mM Hepes, pH 7.5, 150 mM NaCl, 3.5 mM EDTA, and 0.005% Tween 20) and 10 mM glycine/HCl, pH 1.5, was used for regeneration. Data were fitted with the help of the BIAevaluation software version 4.1 (Biacore), on the basis of a 1:1 Langmuir binding model, with simultaneous fitting of the dissociation (k_{off}) and association (k_{on}) rate constants. The kinetic parameters k_{on} and k_{off} were subsequently used to calculate the K_D values.

Temperature-induced Unfolding—CD measurements were performed with a Jasco J715 spectropolarimeter in the far-UV (205–250 nm) region, using a protein concentration of 0.166

mg/ml and 0.1 cm cell path length. A total volume of 300 μl of each sample was heated in 50 mM phosphate (pH 7.0). Heat-induced unfolding was monitored by increasing the temperature from 35 °C to 95 °C at a rate of 1 °C/min, and recording the fluorescence intensity at 205 nm as a function of temperature. Data were acquired with a reading frequency of 1/20 s^{-1}, a 1-s integration time, and a 2 nm bandwidth. Data analysis was performed assuming two-state unfolding mechanisms (21). The reversibility of the unfolding was assessed by recording wavelength scans of the protein at 35 °C, 95 °C and again after cooling down the sample to 35 °C. At each temperature five spectra were measured and averaged.

Enzyme-linked Immunosorbent Assay—To test the residual binding activity after thermal unfolding, the different mutants were incubated at concentrations between 250 nM and 2 μM for 4 h at 90 °C. Maxisorb 96-well plates (Nunc) were coated overnight at 4 °C with human lysozyme or BcII at a concentration of 2 μg/ml in phosphate-buffered saline. Residual protein-binding sites in the wells were blocked for 2 h at room temperature with 1% milk powder in phosphate-buffered saline. After incubation with either untreated or heat-treated and subsequently refolded His-tagged Nanobody, bound protein was detected using a mouse anti-histidine tag antibody (Serotec) followed by an alkaline phosphatase anti-mouse-IgG conjugate (Sigma) and *p*-nitrophenyl phosphate as substrate. The percentage of binding activity restored after temperature unfolding was calculated using triplicates at four different concentrations of Nanobody.

Equilibrium Denaturation Experiments—GdmCl-induced unfolding followed by intrinsic fluorescence measurements was employed to determine the thermodynamic stability. Protein-GdmCl mixtures containing a final protein concentration of 25 μg/ml and denaturant concentrations ranging from 0 to 6.0 M GdmCl were prepared by adding a GdmCl stock solution (7.2 M, in 50 mM phosphate, pH 7.0) to the purified protein (stock 2 mg/ml in phosphate-buffered saline). After overnight incubation at room temperature, the intrinsic fluorescence was measured at 25 °C on an Aminco-Bowman spectrofluorometer from 300 to 400 nm after excitation at a wavelength of 280 nm. The center of spectral mass of each spectrum was calculated as the center of spectral mass = $\Sigma \nu_i \times F_i / \Sigma F_i$, where ν_i is the wave number (*i.e.* inverse wavelength) and F_i is the fluorescence intensity at ν_i (22).

Thermodynamic parameters for chemical unfolding were computed on the assumption of a two-state model for the unfolding reaction, as observed for Nanobodies studied so far (16, 23). On this basis, a first data analysis was performed to obtain the ΔG^0 and m values using a six-parameter equation as previously described by Pace (24) and Santoro and Bolen (25).The concentration of denaturant at which half of the protein is denatured (C_m) has been shown to be the most reproducible value when comparing the stability of wild-type and mutant proteins, because it can be determined quite accurately and is largely insensitive to the unfolding mechanism (26). Transition curves were also analyzed according to Clarke and Fersht (27) and Kellis *et al.* (28) to obtain the C_m and m values. ΔG^0 can then simply be calculated from $\Delta G^0 = m \cdot C_m$. Both fitting procedures resulted in very similar ΔG^0 values, we therefore report only the latter.

Generation of Chimeric Nanobody Constructs—The CDR-H loops from loop donor Nanobodies NbHuL6 (dromedary) and NbHSA (llama) were transferred to the scaffold of h-NbBcII10$_{FGLA}$ (humanized recipient Nanobody) by PCR-based mutagenesis. The sequence of each CDR-H loop from the loop donor Nanobody was encompassed by two primers, one back and one forward primer, containing at the 5′ and the 3′ ends the sequences corresponding to the framework residues of the recipient Nanobody. The chimeras were constructed as described previously with some minor modifications (18). The chimeric Nanobody construct of NbHuL6 on h-NbBcII10$_{FGLA}$ was digested with NcoI and NotI, whereas the chimeric construct with NbHSA as donor Nanobody was digested with HindIII and NotI. Both fragments were cloned in the expression vector pHEN6 (17). The expression yield of both chimeras is comparable to the level of the humanized recipient Nanobody (2 mg/liter of culture).

Crystal Structure Determination—Data for the free form of NbBcII10 (pdb entry 3DWT) were collected at ESRF beamline ID14-2 under cryogenic conditions. The crystals diffract to 2.9-Å resolution. Data were reduced using the HKL suite of programs (29). Molecular replacement was done with the maximum-likelihood based program PHASER (30, 31), which allowed the unambiguous positioning of all eight VHH domains in the asymmetric unit. The framework region of crystal structure of NbBcII10 grafted with the CDR loops from NbLys3 (pdb entry 1ZMY) (18, 32) was used as the starting model. Rounds of simulated annealing refinement and *B*-factor refinement with CNS 1.0 (33) were alternated with manual rebuilding using TURBO (34). NCS restraints were used throughout the refinement, and the mli target function was used. Data collection and refinement statistics are given in Table 1. The final R and R_{free} factors were 0.245 and 0.304, respectively, with the model fitting the electron density very well. Attempts to reduce the R factors by relaxing the NCS restraints or to build different CDR conformations in different monomers were unsuccessful.

X-ray data for the maximally humanized mutant of NbBcII10 (h-NbBcII10$_{FGLA}$, pdb entry 3EAK) were collected at beamline BW7A of the DESY synchrotron, Hamburg, to a resolution of 1.85 Å and processed as for the wild-type data. The same starting model was used for molecular replacement and refinement as for the wild-type NbBcII10 structure to minimize bias. Refinement was carried out using the same protocol as for the wild-type NbBcII10, except that no NCS restraints were applied.

The same protocol was also applied to the partly humanized NbHul6 complex (NbHul6$_{FGLW}$, pdb entry 3EBA), for which the data were also collected on beamline BW7A. The wild-type NbHuL6:HuL complex (pdb entry 1OP9) was used as the starting model for molecular replacement and refinement. All details of data collection and refinement are presented in Table 1.

RESULTS

Humanizing the Framework-2 Region of Nanobodies—Two Nanobodies, NbHuL6 and NbBcII10, with specificity for human lysozyme (HuL) and the β-lactamase BcII of *Bacillus cereus*, respectively, have been selected to determine the involvement of the VHH hallmark amino acid residues in framework-2 on expression yield, affinity, and stability. The

TABLE 1
Crystallographic data and refinement statistics for $NbHuL6_{FGLW}$, NbBcII10, and h-$NbBcII10_{FGLA}$

	$NbHuL6_{FGLW}$	NbBcII10	h-$NbBcII10_{FGLA}$
Space group	$P6_1$	$P2_12_12$	$P2_12_12$
Unit cell	a = b = 63.67 Å c = 119.51 Å	a = 76.72 Å b = 174.71 Å c = 115.53 Å	a = 75.59 Å b = 70.75 Å c = 50.37 Å
Resolution (highest resolution shell)	20.0–1.85 (1.92–1.85) Å	20.0–2.9 (3.0–2.9)	50.0–1.95 (2.02–1.95)
Data collection temperature	100 K	100 K	100 K
Number of measured reflections	107,299 (10208)	238,144 (23075)	129,288 (13187)
Number of unique reflections	23,285 (2320)	34,579 (3402)	20,171 (1998)
Completeness (highest resolution shell)	99.9 (99.9)%	99.9 (100.0)%	99.9 (100.0)
I/σ (I) (highest resolution shell)	14.3 (3.6)	11.4 (2.7)	9.99 (2.3)
R_{merge} (highest resolution shell)	0.069 (0.402)	0.127 (0.485)	0.196 (0.607)
R-factor (highest resolution shell)	0.211 (0.283)	0.245 (0.331)	0.215 (0.237)
R_{free}-factor (highest resolution shell)	0.255 (0.335)	0.305 (0.492)	0.252 (0.265)
Ramachandran plot			
Core region	87.5%	82.5%	87.7%
Additional allowed	12.0%	16.9%	12.3%
Generously allowed	0.5%	0.6%	0.0%
Disallowed	0.0%	0.0%	0.0%
r.m.s.d.			
Bond lengths	0.0058 Å	0.0075 Å	0.0058 Å
Bond angles	1.325°	1.523°	1.37°
pdb entry	3EBA	3DWT	3EAK

NbHuL6 was chosen for this study because of its potential therapeutic relevance, because it stabilizes an unstable human lysozyme mutant that forms fibrils and amyloids (35). The high stability (50.9 kJ mol^{-1}) of NbBcII10 (17) and the successful use of its framework to graft the antigen specificity loops from donor Nanobodies of the VHH subfamily-2 (18), makes it a logical candidate as universal Nanobody scaffold.

The two Nanobodies were mutated by LDA-PCR at the framework-2 hallmark amino acid positions 42, 49, 50, and 52 to the amino acids occurring at those positions in human VH domains, *i.e.* Val42, Gly49, Leu50 and Trp52, [ImMunoGeneTics numbering (imgt.cines.fr)]. These mutants, referred to as $NbHuL6_{VGLW}$ and $NbBcII10_{VGLW}$, respectively, were expressed in the periplasm of *E. coli* and purified by immobilized metal ion chromatography and gel filtration. (Nanobody mutants humanized in framework-2 are designated with a four-letter single letter code for the amino acid at positions 42, 49, 50, and 52; these letters are *italicized* if they correspond to the human sequence at that position). The amount of wild-type protein recovered after size-exclusion chromatography corresponded to 3 mg/liter of culture for NbHuL6 and NbBcII10. The expression yields of the framework-2 humanized proteins were lower: 1 mg/liter of culture for $NbHuL6_{VGLW}$ and 1.8 mg/liter of culture for $NbBcII10_{VGLW}$, probably due to the lower cell density attained after overnight growth or to cell lysis. Both mutant proteins are monomeric, as observed by size-exclusion chromatography (data not shown). However, a delay in elution time from the column is noticed for both framework-2-humanized formats, suggesting nonspecific interaction of the humanized proteins with the gel matrix. This feature was also noted for isolated VH domains of conventional antibodies (13, 23, 36). In addition, the $NbHuL6_{VGLW}$ has a tendency to precipitate upon prolonged storage at 4 °C.

The effect of humanizing the framework-2 region of NbHuL6 and NbBcII10 on the antigen-binding capacity was assessed by surface plasmon resonance. In both cases an increase in the equilibrium dissociation constants was observed (14.6 nM for $NbHuL6_{VGLW}$ compared with 0.32 nM for wild-type NbHuL6 and 16 μM for $NbBcII10_{VGLW}$ compared with 7.4 nM for wild-type NbBcII10 (Tables 2*A* and 3*A*)).

Impact of Trp-118 → Arg Substitution on Expression and Functionality of NbHuL6—Another residue that participates in the interaction with the VL domain and that is highly conserved in conventional VH domain is Trp-118. In ~10% of the Nanobodies this residue, adjacent to the CDR3 loop, is substituted to a more hydrophilic Arg residue (14). This Trp-118 → Arg mutation renders the domain more hydrophilic and was previously shown to have an effect on the expression and solubility of a camelized rabbit VH domain (37). Therefore, the effect of the amino acid residue at position 118 on the expression and functionality of wild-type NbHuL6 and $NbHuL6_{VGLW}$ was investigated.

Introduction of an Arg at position 118 of $NbHuL6_{VGLW}$ leads to a 3-fold improvement of the expression yield, whereas a 2-fold lower expression is observed for the same mutation in NbHuL6. Additionally, the wild-type NbHuL6 with an Arg at position 118 shows a 10-fold drop in affinity (Table 2*A*). The presence of Trp-118 of NbHuL6 had previously been demonstrated to be critical for proper positioning of the third antigen-binding loop (18). This effect on loop organization seems to be independent of the Nanobody hallmark residues in framework-2, because a similar drop (6-fold) in affinity is observed upon mutating the $NbHuL6_{VGLW}$ to include Arg-118.

Impact of Residues 42, 49, 50, and 52 on Biochemical Properties of NbHuL6—Because the effect on affinity is most dramatic for the framework-2-humanized version of NbBcII10, we decided to dissect the contribution of each mutated residue on the biochemical properties of NbHuL6. The residues 49 and 50 are grouped and mutated simultaneously so that we constructed six different mutants between NbHuL6 and $NbHuL6_{VGLW}$, covering all the possible residue combinations at positions 42, 49, 50, and 52. The partially humanized mutants of NbHuL6 were consistently recovered at levels comparable to the wild-type (3–4 mg/liter of culture) with one notable exception for the $NbHuL6_{VGLG}$ mutant having an expression yield of 1.4 mg/liter of culture.

TABLE 2

Kinetic rate and equilibrium dissociation constants, changes in the free energies of unfolding by equilibrium denaturation (*A*) and overview of the heat-induced unfolding experiments (*B*) upon mutation of VHH hallmark residues of NbHuL6

A) NbHuL6[a]	k_{on}	k_{off}	K_D	C_m	*m*-value	ΔG^0	$\Delta\Delta G^{H_2O}$[b] (relative to wild-type)
	$M^{-1}s^{-1}$	s^{-1}	nM	M	$kJmol^{-1}M^{-1}$	$kJmol^{-1}$	$kJmol^{-1}$
FERG	2.39E+06	7.68E-04	0.32	3.02 ± 0.02	13.7 ± 1.0	41.4 ± 3.4	
FER*W*	2.04E+06	6.85E-03	3.36	3.35 ± 0.01	15.5 ± 0.5	51.9 ± 1.9	−10.5
*VE*RG	2.70E+06	1.61E-03	0.60	2.58 ± 0.01	14.4 ± 0.6	37.1 ± 1.8	4.3
VER W	1.01E+06	1.59E-02	15.74	3.05 ± 0.01	16.7 ± 0.7	50.8 ± 2.4	−9.4
F*GL*G	1.42E+06	5.78E-04	0.41	3.39 ± 0.02	19.0 ± 1.9	64.7 ± 6.6	−23.3
F*GL W*	1.63E+06	3.85E-03	2.36	3.83 ± 0.02	14.3 ± 1.1	55.0 ± 4.4	−13.6
*VGL*G	2.58E+06	1.24E-03	0.48	2.95 ± 0.01	19.7 ± 1.3	58.1 ± 3.9	−16.7
VGL W	9.31E+05	1.36E-02	14.61	3.50 ± 0.01	15.4 ± 0.8	54.0 ± 3.1	−12.6
FERG W118R	8.74E+05	2.98E-03	3.41	1.75 ± 0.02	9.0 ± 0.4	15.8 ± 0.9	25.6
VGLW W118R	2.12E+05	1.95E-02	91.98	3.11 ± 0.01	14.9 ± 0.5	46.4 ± 1.7	−5.0

B) NbHuL6[a]	T_m	Reversibility	restored activity
	°C	%	%
FERG	79.7 ± 0.2	93.3	86.8
FER*W*	84.2 ± 0.5	93.4	ND
*VE*RG	76.2 ± 0.2	93.0	58.8
VER W	79.4 ± 0.2	92.6	100
F*GL*G	82.5 ± 0.3	96.3	64.9
F*GL W*	ND[c]	103.1	100
*VGL*G	78.4 ± 0.2	81.6	65.4
VGL W	79.5 ± 0.3	66.7	79.9
FERG W118R	70.0 ± 0.1	69.9	58.4
VGLW W118R	79.9 ± 0.2	86.3	55.5

[a] Partially humanized mutants in framework-2 are designated with a four-letter label referring to the residues at, respectively, positions 42, 49, 50, and 52. The human hallmark residues at these positions are in italic font.
[b] $\Delta\Delta G^0 = \Delta G^0$ (wild type) − ΔG^0 (mutant) (27, 28).
[c] ND, not determined.

TABLE 3

Kinetic rate and equilibrium dissociation constants, changes in the free energies of unfolding by equilibrium denaturation (*A*) and overview of the heat-induced unfolding experiments (*B*) upon humanization of NbBcII10 and of chimeras based on the h-NbBcII10$_{FGLA}$ scaffold

A)	k_{on}	k_{off}	K_D	C_m	*m*-value	ΔG^0	$\Delta\Delta G^{H_2O}$[a] (relative to wild type)
	$M^{-1}s^{-1}$	s^{-1}	nM	M	$kJmol^{-1}M^{-1}$	$kJmol^{-1}$	$kJmol^{-1}$
NbBcII10	4.87E+06	3.61E-02	7.41	3.17 ± 0.01	16.1 ± 0.6	50.9 ± 2.1	
NbBcII10$_{VGLW}$	1.51E+04	2.42E-01	16E+03	ND[b]	ND	ND	
NbBcII10$_{FGLA}$	7.98E+06	3.50E-02	4.39	3.61 ± 0.01	20.4 ± 1.6	73.7 ± 6.1	−22.8
h-NbBcII10	3.69E+06	4.45E-02	12.06	2.95 ± 0.01	14.9 ± 1.1	43.9 ± 3.4	7.0
h-NbBcII10$_{FGLA}$	3.67E+06	3.19E-02	8.69	3.38 ± 0.02	17.2 ± 1.1	58.3 ± 3.7	−7.4
NbHSA	2.83E+06	2.08E-02	7.35	2.46 ± 0.01	14.9 ± 1.2	34.1 ± 2.3	
h-NbBcII10$_{FGLA}$ S-S-S	4.50E+06	1.56E-02	3.47	2.03 ± 0.01	15.6 ± 0.8	31.7 ± 1.9	2.4
NbHuL6	2.39E+06	7.68E-04	0.32	3.02 ± 0.02	13.7 ± 1.0	41.4 ± 3.4	
h-NbBcII10$_{FGLA}$ L-L-L	1.66E+06	1.66E-03	1.00	3.80 ± 0.01	12.3 ± 0.4	46.9 ± 1.8	−5.5

B)	T_m	Reversibility	Restored activity
	°C	%	%
NbBcII10	77.5 ± 0.2	41.9	59.6
NbBcII10$_{FGLA}$	79.6 ± 0.2	39.3	35.5
h-NbBcII10	72.0 ± 0.2	35.3	1.5
h-NbBcII10$_{FGLA}$	74.3 ± 0.3	8.1	0.4
h-NbBcII10$_{FGLA}$ S-S-S	63.4 ± 0.1	19.3	ND
NbHuL6	79.7 ± 0.2	93.3	86.8
h-NbBcII10$_{FGLA}$ L-L-L	82.1 ± 0.3	68.1	ND

[a] $\Delta\Delta G^0 = \Delta G^0$ (wild type) − ΔG^0 (mutant) (27, 28).
[b] ND, not determined.

To get a better view on the involvement of each of the humanizing mutations on the kinetic parameters, the affinity of each partially humanized mutant of NbHuL6 was determined. The most obvious and consistent effect upon mutating Gly to Trp at position 52 is a 6- to 10-fold increase in the kinetic off-rate (Table 2*A* and Fig. 2). The concomitant increase in K_D value is even more accentuated when a Val is located at position 42. This leads to the proposal that residue 52 is essential for high affinity antigen binding; most probably in conjunction with the residue at position 42. Only minor differences in affinity were observed when mutating the residues at positions 49 and 50.

The impact of the different mutations in framework-2 on the stability of NbHuL6 was assessed by determining the free energy of unfolding of all mutants from denaturant-induced unfolding and refolding experiments (Table 2*A*). The unfolding is completely reversible for all variants, because the fluorescence spectra measured after refolding are indistinguishable from those of the native states before unfolding (data not shown). The *m* values around 15 $kJmol^{-1}M^{-1}$ are in the range expected for proteins of this size (14–15 kDa) (38). A single unfolding transition was observed, indicating a cooperative two-state unfolding of the Nanobodies (Fig. 3*A*). The mutations Glu-49 → Gly and Arg-50 → Leu result in a notable increase in protein stability, especially when another Gly occupies position 52 (Table 2*A* and Fig. 3, *B* and *C*). Conversely, a loss of stability was observed upon mutation of Phe to Val at position 42.

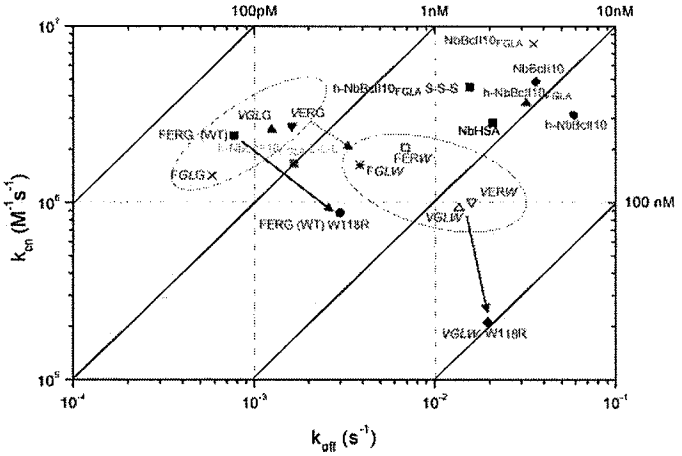

FIGURE 2. **Rate plane with isoaffinity diagonals plot for the different mutants of NbHuL6 (*red*) and NbBcII10 (*purple*) and the chimeric constructs h-NbBcII10$_{FGLA}$ L-L-L (*green*) and h-NbBcII10$_{FGLA}$ S-S-S (*blue*) as determined by surface plasmon resonance.** *Arrows* represent the decrease in affinity upon mutation of Gly-52 → Trp (*dotted*) and Trp-118 → Arg (*solid*). Partially humanized mutants in framework-2 are designated with a *four-letter label* referring to the residues at, respectively, positions 42, 49, 50, and 52. The human hallmark residues at these positions are in *italics*.

Temperature-induced unfolding followed by CD spectroscopy largely confirms these results (Table 2*B*). For all the different variants of NbHuL6 a single transition was observed, consistent with two-state folded-unfolded behavior (Fig. 4*A*). As expected, a large proportion (>90%) of the native ellipticity was recovered upon cooling the samples from 95 °C to 35 °C, with exception for the NbHuL6$_{VGLG}$ and NbHuL6$_{VGLW}$ formats. This indicates that the domains reversibly refold upon cooling, a well established property of Nanobodies and engineered human VH single-domain antibodies (16, 23, 36). However, this observation contrasts with a reduced antigen-binding capacity of some of the mutants after heat treatment (Table 2*B*).

Structural Consequences of Humanizing NbHuL6—The structure of wild-type NbHuL6 in complex with human lysozyme has been described previously (35) (pdb entry 1OP9). The partly humanized version of NbHuL6 (NbHuL6$_{FGLW}$) was crystallized in complex with its antigen in a different crystal form (Fig. 5, *A* and *B*). The antibody domains within the different crystal forms superimpose with an r.m.s.d. of 0.75 Å for 121 Cα atoms, significantly higher than the 0.42 Å obtained when superimposing the two lysozyme molecules (which defines the effect of comparing two different crystal forms). The per residue r.m.s.d. plot shows a single peak for residues 45–50 upon a base line of ~0.6 Å r.m.s.d. for all other residues. Although this deviation coincides with the region where the mutations where inserted, it appears to be rather attributed to crystal packing effects (Fig. 5*D*). There are no prominent differences in the CDR1 and CDR2 loops, but the CDR3 loop is slightly shifted by the presence of Trp at position 52. Its bulky side-chain forces the Leu 112.2 to reorient itself, which in turn pushes against the side chain of Trp 111.1 (Fig. 5*C*).

The surface area of the antibody-antigen interface employed for the association of the antigen to the wild type or the partly humanized NbHuL6$_{FGLW}$ is very similar and occurs via the same contacts, despite a 9.2° rigid body rotation in the antigen position (around the CDR3 loop). Such rigid body rotations have been observed for other antibody complexes for which different polymorphs are available (39). They most likely represent the flexibility of such complexes in solution, of which different substrates are selected for by the crystal lattice. Of interest is that the antibody-antigen interactions are overwhelmingly dominated by interactions involving side chains of NbHuL6 with only very few main-chain atoms involved. This contrasts to earlier observations that suggested that the high affinity of heavy-chain antibodies might in part be due to a high tendency to recruit the polypeptide backbone as this would reduce the entropy penalty of the association (40).

Humanization by Veneering of the Complete Framework of NbBcII10—Apart from the Nanobody hallmark residues in framework-2, other amino acids differences occur between the VHH framework and the VH framework of a conventional antibody at various positions. To obtain a single-domain antibody fragment with the highest possible similarity to human germ line sequences, we also humanized these residues using the human germ line DP-47 as a reference (41) (Fig. 1*B*). DP-47 belongs to the VH family III, which also includes the camelid VHH domains and is well expressed/displayed in bacterial/phage systems (42). The VH family III occurs in antibodies against a wide variety of different antigens.

NbBcII10 was preferred for this analysis because of its high conformational stability (50.9 kJ/mol ± 2.1) and the successful use of its framework in several loop-grafting experiments (18). At first, eleven camelid VHH framework residues outside framework-2 of NbBcII10 were humanized to mimic the DP-47 sequence (Ser-12 → Leu, Ala-15 → Pro, Thr-24 → Ala, Ala-83 → Ser, Val-87 → Leu, Thr-88 → Tyr, Asn-93 → Ser, Lys-95 → Arg, Pro-96 → Ala, Ile-101 → Val, and Gln-123 → Leu) (h-NbBcII10). These solvent-exposed residues are expected to have only minor influence on the CDR conformation (43, 44), which is confirmed by the wild-type-like binding behavior of h-NbBcII10 (Table 3*A* and Fig. 2). However, this resurfacing affects the stability of NbBcII10, because its melting point decreases from 77.5 °C to 72.0 °C for h-NbBcII10.

We demonstrated earlier the severe impact of the humanization of framework-2 on the antigen-binding capacity of NbBcII10. Our analysis on NbHuL6 demonstrates that this effect was mainly attributed to the residues at positions 42 and 52. Therefore only the residues at positions 49 and 50 in framework-2 were changed to their human counterpart in NbBcII10 and h-NbBcII10. We then compared the biochemical properties of NbBcII10$_{FGLA}$ and h-NbBcII10$_{FGLA}$, respectively, and observed a considerable gain in thermodynamic as well as thermal stability, whereas the antigen-binding capacity and solubility are preserved (Table 3, *A* and *B*, and Fig. 2). The increase in stability even compensates for the loss of stability observed for the veneered h-NbBcII10. As for NbHuL6, the mutations at positions 49 and 50 cause a more sticky behavior of the mutated proteins, resulting in a longer retention time on the size-exclusion chromatography column. Strikingly, the maximal humanization of the NbBcII10 resulted in a complete loss of the reversible refolding and binding activity after heat treatment (Table 3*B*). This seems to be communally attributed to the mutations spread throughout the entire scaffold region of NbBcII10 and is not only confined to those of framework-2.

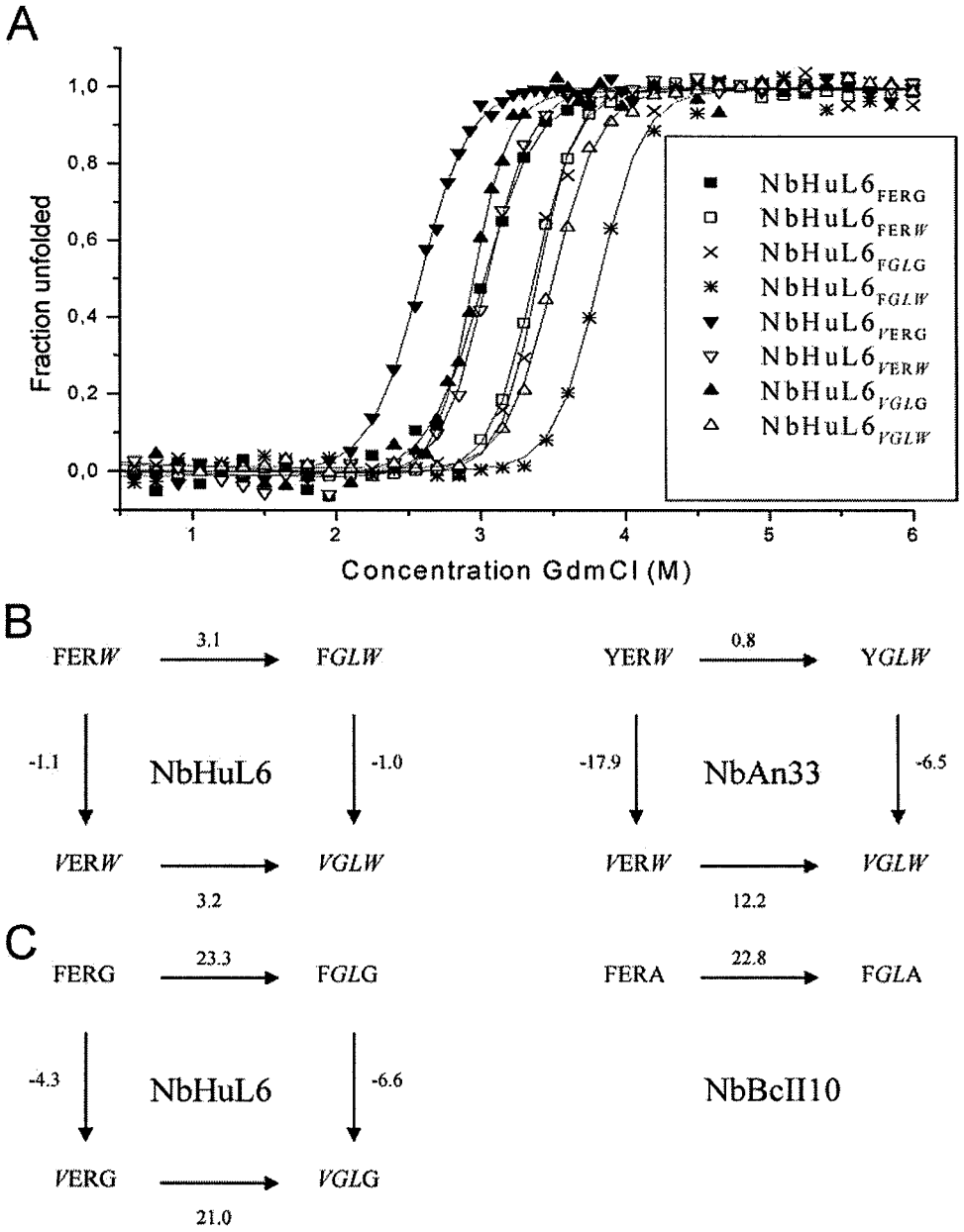

FIGURE 3. *A*, fraction of Nanobody unfolded, f_U, as a function of GdmCl concentration of the partially humanized mutants of NbHuL6. Curves are normalized to the fraction of unfolded protein. Double mutant cycle at Phe/Tyr-42 → Val and Glu-49 → Gly/Arg-50 → Leu with Trp-52 (*B*) and Gly/Ala-52 (*C*). The numeric values represent the unfolding free energies in kJ/mol as recovered from Table 2 for NbHuL6, Table 3 for NbBcII10, and according to Conrath *et al.* (13) for NbAn33. Partially humanized mutants in framework-2 are designated with a *four-letter label* referring to the residues at, respectively, positions 42, 49, 50, and 52. The human hallmark residues at these positions are in *italics*.

dinates in the wild-type structure), similar to the situation in NbHuL6. Pairwise r.m.s.d. plots as a function of residue number show that the corresponding structural adaptations are spread over the entire structure rather than being located in specific regions, in agreement with the thirteen mutations being distributed over the entire sequence. Nevertheless, somewhat larger deviations are observed for the N terminus, CDR2, and residues 80–88. These differences are, however, difficult to link to specific mutations and may, at least in part, be a consequence of different crystallization conditions and crystal lattice interactions.

The crystal structure of the h-NbBcII10$_{FGLA}$ was superimposed on the single-domain human VH structures 1OHQ and 3B9V from Jespers, *et al.* (45) and Barthelemy, *et al.* (36), respectively, to assess the structural effect of the humanized sequences in our Nanobody. With the exception of the residues Ser-83 and Val-101, where a 120° turned rotamer of the side chain was noticed without further effect on surrounding residues, all other amino acids had an identical positioning.

Grafting Experiments on the Humanized h-NbBcII10$_{FGLA}$—The identification of a highly stable, humanized Nanobody scaffold that allows grafting of the antigen-binding loops of single-domain antibodies is an ultimate goal. For h-NbBcII10$_{FGLA}$ to be a good universal scaffold we need to demonstrate that its maximally humanized framework serves as a universal acceptor for loop grafting and concomitantly for transfer of antigen specificity. We therefore constructed two Nanobody chimeras by CDR grafting and analyzed their biophysical properties. As mentioned before, NbHuL6 is a member of the dromedary subfamily-2, whereas the llama NbHSA belongs to the VHH subgroup C according to the classification of Achour *et al.* (3). The latter Nanobody was chosen to demonstrate the tolerance to transfer the antigen specificity and affinity of a non-dromedary VHH to our humanized dromedary VHH scaffold. Grafting the CDRs of NbHSA and NbHuL6 on the framework of h-NbBcII10$_{FGLA}$ to generate h-NbBcII10$_{FGLA}$ S-S-S and h-NbBcII10$_{FGLA}$ L-L-L, respectively, had no significant effect on the expression and the affinity of the recombinant proteins (Table 3*A* and Fig. 2). The thermodynamic stability of the

Structural Effects of Humanizing NbBcII10—The crystal structure of wild-type and maximally humanized NbBcII10 (h-NbBcII10$_{FGLA}$) were determined to 2.9 Å and 2.1 Å resolution, respectively (Fig. 6, *A* and *B*).

The maximally humanized mutant of NbBcII10 crystallizes with two molecules in the asymmetric unit. Both molecules are very similar (r.m.s.d. 0.37 Å for 128 Cα atoms). All mutated residues have their side-chain solvent exposed on the surface of the molecule and provoke a minimal structural adaptation of the protein. The mutant structures are nevertheless distinct from the wild-type structures with r.m.s.d. values between 0.77 and 0.88 Å for 125 Cα atoms (three residues have missing coor-

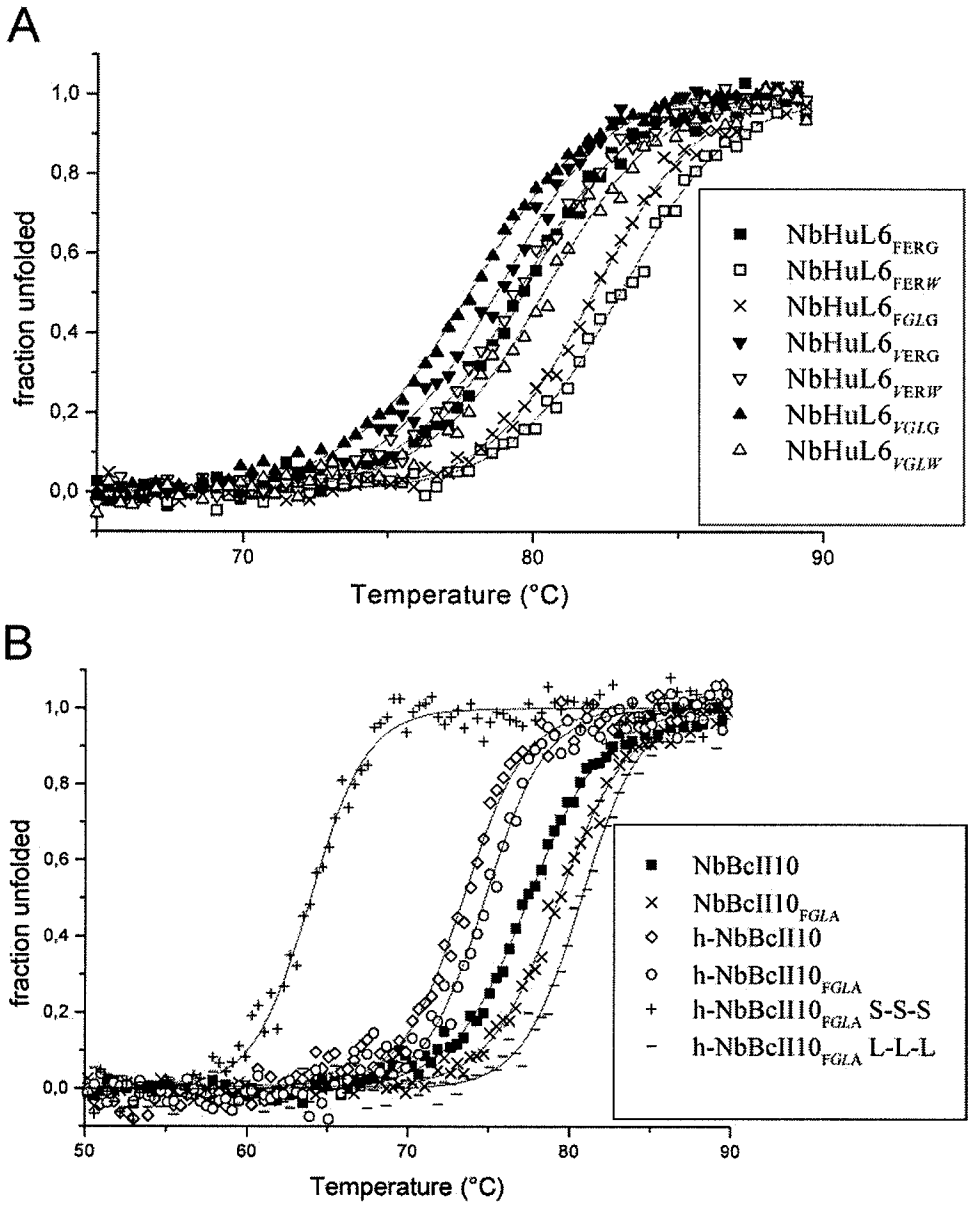

FIGURE 4. **Temperature-induced unfolding transitions of (*A*) NbHuL6 and (*B*) NbBcII10 variants monitored at 205 nm.** Curves are normalized to the fraction of unfolded protein. Partially humanized mutants in framework-2 are designated with a *four-letter label* referring to the residues at, respectively, positions 42, 49, 50, and 52. The human hallmark residues at these positions are in *italics*.

h-NbBcII10$_{FGLA}$ S-S-S was slightly decreased compared with that of the original clone, whereas in the case of hNbBcII10$_{FGLA}$ L-L-L, the stability was higher than for NbHuL6. This result is confirmed by the heat-induced unfolding experiments showing a small increase in T_m value of h-NbBcII10$_{FGLA}$ L-L-L (Table 3*B*). In addition, the reversible refolding after heat-induced unfolding of h-NbBcII10$_{FGLA}$ was partially restored after grafting the CDR loops of NbHuL6. It corroborates that, apart from the scaffold, the CDRs also contribute to this particular property of camelid single-variable domains.

DISCUSSION

Camelid single-domain antibody fragments or Nanobodies have a high potential for biotechnological and medical applications because of their small size, good stability, high antigen affinity and specificity, and improved solubility. Due to their small size and the high degree of identity of their framework to the human VH framework of family III, Nanobodies are expected to exhibit a low immunogenicity (14). Nevertheless, for tumor therapy the perception is that the Nanobody needs to be humanized to a maximal degree, evidently without compromising on their expression level, affinity, solubility, and stability.

The most remarkable differences between Nanobodies and human VH domains are the adaptations in the framework-2 region. Most of these mutations involve a substitution from a hydrophobic to a hydrophilic residue and are considered to be important for the solubility of the isolated Nanobody (12, 13). Indeed, human VH domains occur in nature only in complex with a VL domain, and the removal of this VL domain would expose a large hydrophobic surface to the solvent. Therefore, most isolated VH domains have a pronounced tendency to aggregate (46). Consequently, it is crucial to understand the influence of each of these framework-2 substitutions on the biophysical properties of Nanobodies to produce the most optimal single-domain antibody format. To date, most studies attempting to unravel the function of these VHH hallmark residues have focused on the partial camelization of conventional VH single domains to exploit the favorable properties of Nanobodies (12, 37, 47, 48). This approach achieved only limited success as camelizing mutations on human or mouse VH was shown to be thermodynamically destabilizing due to framework deformations and did not completely eliminate the tendency to dimerize and aggregate (49–51). In another approach, Barthelemy *et al.* (36) introduced a guided molecular evolution technique to mutagenize a human VH into a stabilized, reversibly refolding, better expressing, and autonomous single-domain antibody fragment. Here we start from a properly behaving dromedary-derived Nanobody and propose a strategy to humanize this single-domain antibody. The advantage of humanized Nanobodies over camelized human VHs is that VHH domains evolved naturally, matured in the absence of a VL partner and will therefore behave as soluble, strictly monomeric, specific single domains. Other adaptations outside the framework-2, spread over the entire VHH

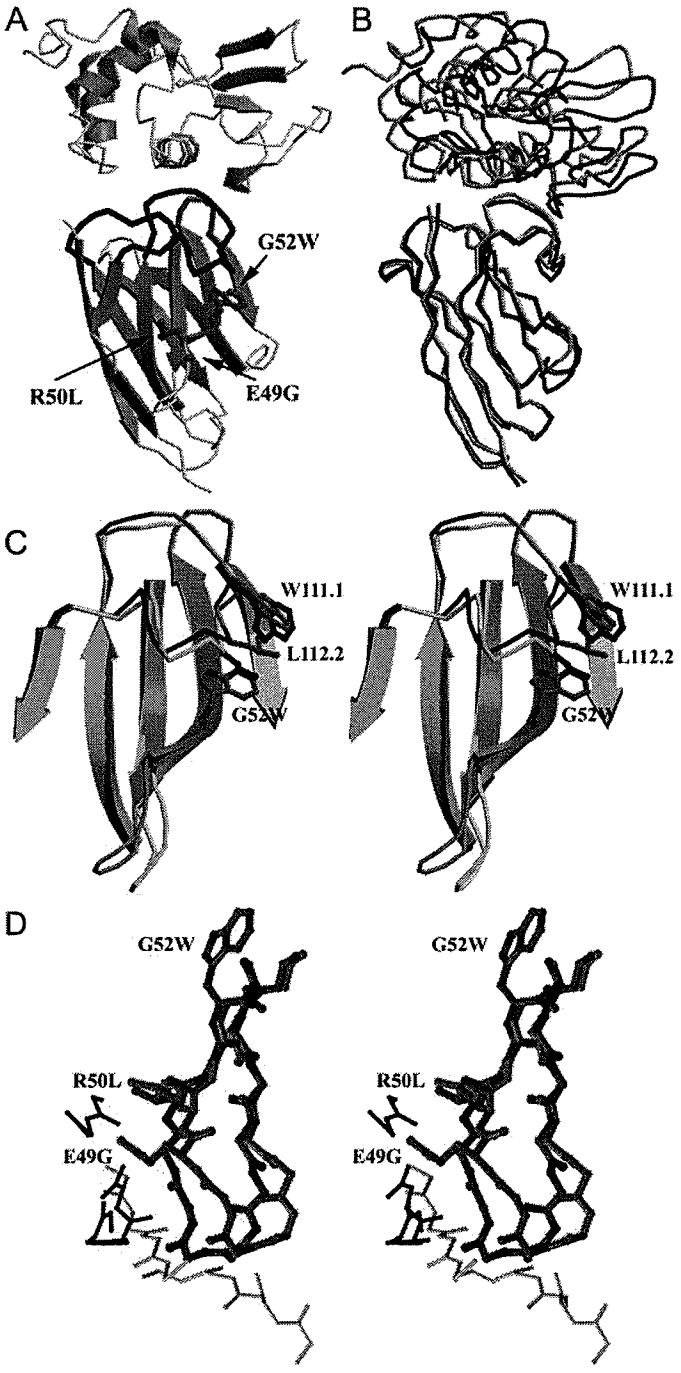

FIGURE 5. **The NbHuL6-HuL complex.** *A, ribbon diagram* of the structure of the NbHuL6$_{FGLW}$ mutant in complex with human lysozyme. The antibody is drawn in *purple* and the lysozyme molecule in *orange*. Residues Gly-49, Leu-50, and Trp-52 are drawn as *ball-and-stick*. The three CDR loops are *highlighted*: CDR1 in *blue*, CDR2 in *green*, and CDR3 in *red*. *B*, superposition of the wild-type complex (Nanobody in *dark blue* and lysozyme in *red*) on the mutant complex of NbHuL6$_{FGLW}$ (Nanobody in *light blue*, lysozyme in *orange*). The 9.2° rigid body rotation of the antigen is clearly noted. *C*, structural effects of the Gly-52 → Trp mutation. *Stereo ribbon* representation of the superposition of wild-type NbHuL6 (*gray backbone* and *black side chains*) on the mutant NbHuL6$_{FGLW}$ (*colored*). The bulky side chain of Trp-52 pushes against Leu 112.2, which in turn pushes against Trp 111.1, resulting in a small but significant distortion in the CDR3 conformation. This is the most likely cause of the rigid body rotation of the antigen relative to the Nanobody in the mutant complex. *D*, stereo view of a superposition of the mutant NbHuL6$_{FGLW}$ colored according to atom type and the wild-type NbHuL6 (*green*). Conformational changes involve framework-2. Shown are the backbone of residues 41–53 and the side chains of residues Gly-52 → Trp, Glu-49 → Gly, and Arg-50 → Leu. Relevant crystal packing interactions for the mutant are drawn in *black* and for the wild-type in *gray*.

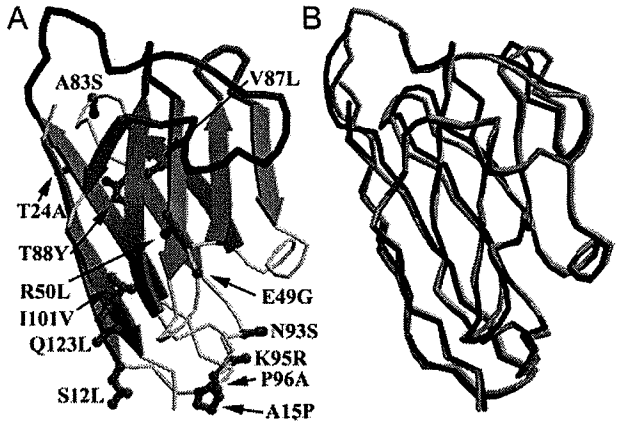

FIGURE 6. *A, ribbon diagram* of the structure of the maximally humanized h-NbBcII10$_{FGLA}$ mutant. The humanized residues are drawn as *ball-and-stick*. The three CDR loops are *highlighted*: CDR1 in *blue*, CDR2 in *green*, and CDR3 in *red*. *B*, superposition of the wild-type NbBcII10 (*dark blue*) on the mutant h-NbBcII10$_{FGLA}$ (*light blue*).

sequence, probably assist in obtaining the best possible single-domain format.

In a previous study, we assessed the effect of mutating the Nanobody hallmark amino acid in framework-2 on the stability, solubility, and loop conformation of NbAn33 (13). However, this NbAn33 (with Tyr-42 and Trp-52) belongs to the rare VHH subfamily-5, whereas the majority of the dromedary-derived Nanobodies belong to the subfamily-2. In addition, the short CDR3 loop of NbAn33 does not fold over the "former VL side" as observed for Nanobodies with longer CDR3 loops (15, 52, 53). Consequently, NbAn33 was more straightforward to humanize in contrast to the abundant subfamily-2 Nanobodies with longer CDR3.

In this study we analyzed the effect of the substitutions of residues Phe-42, Glu-49, Arg-50, and Gly-52 in framework-2 to their human counterpart on expression, affinity, stability, and biophysical properties of NbHuL6 and NbBcII10, representative members of VHH subfamily-2. Nanobodies of this VHH subfamily encompass 75% of all dromedary antigen-specific Nanobodies (2). These results allow us to determine which residues in framework-2 can be humanized without hampering the functionality of these single-domain antibodies. Thereafter, we humanized the remaining Nanobody scaffold to generate a more human-like generic VHH-derivative with maximal retention of its original Nanobody beneficial properties.

The important increase in stability of NbHuL6 and NbBcII10 upon humanization of residues 49 and 50, especially when the residue at position 52 is not mutated to the VH hallmark residue (*i.e.* Trp) is a striking result. A similar effect on stability had already been noticed for NbAn33, although in this case the increase in stability upon mutation of residues 49 and 50 is less pronounced possibly, because the natural residue at position 52 is already occupied by a VH-like Trp (13). These results are consistent with studies on camelized VHs, where mutations in framework-2 usually lead to a decrease in domain stability (12). The residues at positions 49 and 50 are always charged residues in the VHH format, which reduces the exposed hydrophobic area of the former VL interface and renders the domain more hydrophilic. A reasonable explanation is that the VHH domain

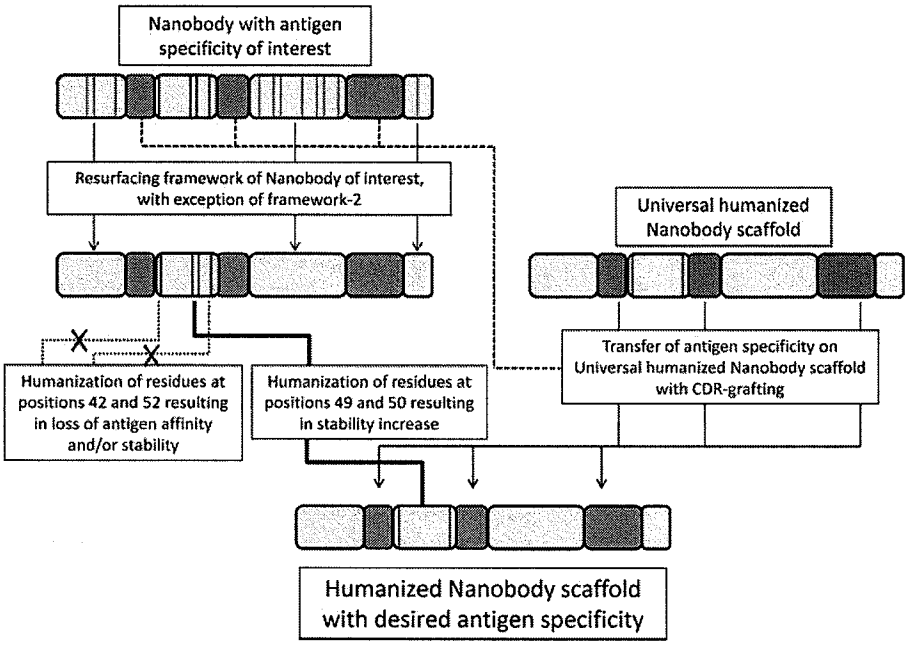

FIGURE 7. **Schematic overview of the Nanobody humanization strategy.** *Left panel*: resurfacing the framework of a Nanobody with an antigen specificity of interest. Residues 42 and 52 are maintained due to their impact on antigen affinity and/or stability. *Right panel*: grafting antigen specificity loops from donor Nanobody on the universal humanized Nanobody scaffold. Solvent-exposed residues in framework (*blue lines*), VHH hallmark residues in framework-2 (*black lines*), non-mutated VHH hallmark residues (*red lines*).

concedes in stability by replacing non-polar with polar residues at positions 49 and 50 to enhance its solubility. Therefore, camelizing the Gly-49 and Leu-50 of a VH sequence will provoke a domain destabilization, whereas humanization of the Glu-49 and Arg-50 of a VHH will generate a stabilized variable domain. Furthermore, the monomeric state of the Nanobodies is not compromised by the Glu-49 → Gly and Arg-50 → Leu mutations as observed from the single symmetrical elution peak on size-exclusion chromatography, despite a more sticky behavior on the gel matrix. Several studies already demonstrated that other inherent features in the sequences of single- domain antibodies of *Camelidae* also contribute to this soluble and monomeric behavior (54, 55). Moreover, the mutations at positions 49 and 50 seem to be completely neutral for the antigen-binding capacity of the Nanobodies we studied.

Conversely, the nature of residue 52 appears to affect strongly the antigen-binding capacity of NbHuL6 and NbBcII10. The most probable explanation for this effect is that the replacement of a Gly by the bulky side chain of Trp-52 provokes a conformational shift of the CDR3 loop as seen in the crystal structure with $NbHuL6_{FGLW}$ (Fig. 5*C*). This confirms the importance of the Gly-52 in Nanobodies for proper positioning of the third antigen-binding loop (13). Indeed, it seems that Gly-52 was evolutionary introduced into the many VHH germ line genes to allow positioning of the long CDR3 over the former VL side. However, the occurrence of Gly-52 might be at the expense of the domain stability, as demonstrated by the higher C_m and T_m values when a Trp substitutes Gly at this position (T_m and C_m values of 84.2 °C and 3.35 M, respectively, for the $NbHuL6_{FERW}$ format compared with 79.7 °C and 3.02 M for wild type).

The exact role of Phe-42 is less straightforward. In this study, substitution by Val-42 changes the expression yield, binding capacity and stability, although these effects don't seem to be solely attributable to this single mutation but rather result from synergy with surrounding residues at positions 49, 50, and 52. In conventional VH domains, the hydrophobic side chains of Val-42, Leu-50, Trp-52, and Trp-118 cluster and create the interaction surface for the VL domain. The conserved use of a bulky aromatic residue (Phe in VHH subfamily-2) is at first sight rather surprising, but crystal structures reveal that the side chain of Phe-42 fills a hydrophobic pocket created by the bulge at Gly-52 and the side chains of Tyr-103, Trp-118, and the CDR3 (32). This Val-42 → Phe substitution presumably stabilizes the "former" VL interface and might compensate partially for the stability loss caused by the solubility increasing substitutions Gly-49 → Glu and Leu-50 → Arg. This hypothesis is in agreement with the structure of the camelized human VH fragment, VH-P8, where Val maintained at position 42 causes a distortion of the former VL-side (50). In conclusion, Phe-42 seems to be essential to maintain the structural integrity and the correct global fold of the Nanobody scaffold. This is confirmed by the better expression levels and the higher stability of the domains with a Phe instead of a Val located at position 42. As a result the crystal structure could be determined for the $NbHuL6_{FGLW}$ format, which was not possible for the $NbHuL6_{VGLW}$ mutant, because of low expression yield and aggregation at lower concentrations.

The Trp-118 → Arg mutation increases the expression level of $NbHuL6_{VGLW}$. A similar significant yield improvement was previously observed for both the wild-type and the framework-2-humanized format of NbAn33. This emphasizes the critical role of Arg-118 for the expression of Nanobodies. However, the presence of a Trp at this position in most Nanobodies cannot be substituted by Arg because of its detrimental influence on the antigen affinity of these Nanobodies, probably by hampering the proper positioning of the third antigen-binding loop.

In summary, in this part of our study we demonstrated that the conserved Nanobody residues at positions 42 and 52 have a major impact on the integrity of the antigen interaction. Surprisingly, humanizing the residues at positions 49 and 50 stabilizes the Nanobodies, without affecting dramatically their solubility and antigen affinity.

We further focused on humanizing the remaining framework to mimic the human VH sequence as much as possible. The sequence DP-47, derived from human subgroup III, was chosen as template. This choice corresponds to the most commonly used VH subgroup in the natural repertoire of human antibodies (56, 57). In addition there is an interesting correla-

tion between stability and framework-1 classification (58). The most stable human VH3 domain belongs to structural subtype II, as do DP-47 and the Nanobodies. Eleven additional residues outside framework-2 were mutated to their human counterpart in the framework of NbBcII10 (h-NbBcII10). These mutations do not significantly affect the antigen-binding capacity of the Nanobody but cause a decrease in expression yield and stability of the single domain. This was anticipated, because some of the substituted residues (*e.g.* Ala-83 → Ser, Lys-95 → Arg, and Gln-123 → Leu) were previously identified as foldability/stability determinants of water-soluble llama VH fragments (55). However, the beneficial effects of humanizing the residues at positions 49 and 50 were sufficient to compensate for this loss in stability. As for NbHul6, these mutations render the scaffold more sticky on the gel matrix, however, without affecting its monomeric state. In addition, the successful transfer of antigen specificity of loop donors onto the framework of h-NbBcII10$_{FGLA}$ demonstrates that this scaffold can be used as a universal humanized acceptor for loop grafting.

All these data allow us to propose two strategies to manufacture a humanized version of a Nanobody with maximal retention of stability and antigen-binding characteristics (Fig. 7). For every *in vivo* affinity-matured Nanobody with an antigen specificity of interest that needs to be humanized we advice to graft its antigen-binding loops into our universal humanized Nanobody scaffold (h-NbBcII10$_{FGLA}$). This will normally guarantee a good expression, stability, and solubility of the chimeric Nanobody with retention of the antigen specificity and affinity of the loop donor VHH. However, because particular framework residues might be directly or indirectly involved in antigen interaction, *e.g.* by presenting the CDR loops in the proper architecture for antigen binding, the simple transfer of the CDRs-only onto the universal humanized Nanobody scaffold may disturb the proper CDR positioning, leading to unacceptable affinity loss. In these cases, the framework of the isolated Nanobody should be resurfaced to minimize the number of camelid Nanobody-specific residues. The humanization of residues in framework regions 1, 3, and 4 will have a minimal effect, whereas the mutations of amino acids in framework-2 at positions 49 and 50 to Gly and Leu, respectively, will even stabilize the autonomous domain (at the expense of solubility and reversibly unfolding). The humanization of amino acids at positions 42 and 52 in framework-2 is discouraged due to their proven involvement in antigen affinity and stability of Nanobodies.

Finally, we anticipate that our universal humanized Nanobody h-NbBCII10$_{FGLA}$ is an excellent candidate to construct a single-framework, synthetic library by introducing variability into its CDRs.

REFERENCES

1. Hamers-Casterman, C., Atarhouch, T., Muyldermans, S., Robinson, G., Hamers, C., Songa, E. B., Bendahman, N., and Hamers, R. (1993) *Nature* **363,** 446–448
2. Nguyen, V. K., Hamers, R., Wyns, L., and Muyldermans, S. (2000) *EMBO J.* **19,** 921–930
3. Achour, I., Cavelier, P., Tichit, M., Bouchier, C., Lafaye, P., and Rougeon, F. (2008) *J. Immunol.* **181,** 2001–2009
4. Harmsen, M. M., Ruuls, R. C., Nijman, I. J., Niewold, T. A., Frenken, L. G., and de Geus, B. (2000) *Mol. Immunol.* **37,** 579–590
5. Arbabi Ghahroudi, M., Desmyter, A., Wyns, L., Hamers, R., and Muyldermans, S. (1997) *FEBS Lett.* **414,** 521–526
6. Baral, T. N., Magez, S., Stijlemans, B., Conrath, K., Vanhollebeke, B., Pays, E., Muyldermans, S., and De Baetselier, P. (2006) *Nat. Med.* **12,** 580–584
7. Cortez-Retamozo, V., Backmann, N., Senter, P. D., Wernery, U., De Baetselier, P., Muyldermans, S., and Revets, H. (2004) *Cancer Res.* **64,** 2853–2857
8. Huang, L., Reekmans, G., Saerens, D., Friedt, J. M., Frederix, F., Francis, L., Muyldermans, S., Campitelli, A., and Hoof, C. V. (2005) *Biosens. Bioelectron.* **21,** 483–490
9. Rothbauer, U., Zolghadr, K., Muyldermans, S., Schepers, A., Cardoso, M. C., and Leonhardt, H. (2008) *Mol. Cell Proteomics.* **7,** 282–289
10. Saerens, D., Frederix, F., Reekmans, G., Conrath, K., Jans, K., Brys, L., Huang, L., Bosmans, E., Maes, G., Borghs, G., and Muyldermans, S. (2005) *Anal. Chem.* **77,** 7547–7555
11. Muyldermans, S., Atarhouch, T., Saldanha, J., Barbosa, J. A., and Hamers, R. (1994) *Protein Eng.* **7,** 1129–1135
12. Davies, J., and Riechmann, L. (1994) *FEBS Lett.* **339,** 285–290
13. Conrath, K., Vincke, C., Stijlemans, B., Schymkowitz, J., Decanniere, K., Wyns, L., Muyldermans, S., and Loris, R. (2005) *J. Mol. Biol.* **350,** 112–125
14. Harmsen, M. M., and de Haard, H. J. (2007) *Appl. Microbiol. Biotechnol.* **77,** 13–22
15. Desmyter, A., Decanniere, K., Muyldermans, S., and Wyns, L. (2001) *J. Biol. Chem.* **276,** 26285–26290
16. Dumoulin, M., Conrath, K., Van Meirhaeghe, A., Meersman, F., Heremans, K., Frenken, L. G., Muyldermans, S., Wyns, L., and Matagne, A. (2002) *Protein Sci.* **11,** 500–515
17. Conrath, K. E., Lauwereys, M., Galleni, M., Matagne, A., Frere, J. M., Kinne, J., Wyns, L., and Muyldermans, S. (2001) *Antimicrob. Agents Chemother.* **45,** 2807–2812
18. Saerens, D., Pellis, M., Loris, R., Pardon, E., Dumoulin, M., Matagne, A., Wyns, L., Muyldermans, S., and Conrath, K. (2005) *J. Mol. Biol.* **352,** 597–607
19. Chen, Z., and Ruffner, D. E. (1998) *Nucleic Acids Res.* **26,** 1126–1127
20. Gasteiger, E., Gattiker, A., Hoogland, C., Ivanyi, I., Appel, R. D., and Bairoch, A. (2003) *Nucleic Acids Res.* **31,** 3784–3788
21. Pace, C. N., and Scholtz, J. M. (1997) in *Protein Structure, A practical Approach* (Creighton, T. E., ed) pp. 299–321, Oxford University Press, New York
22. Royer, C. A. (1995) *Methods Mol. Biol.* **40,** 65–89
23. Ewert, S., Cambillau, C., Conrath, K., and Pluckthun, A. (2002) *Biochemistry* **41,** 3628–3636
24. Pace, C. N. (1990) *Trends Biotechnol.* **8,** 93–98
25. Santoro, M. M., and Bolen, D. W. (1988) *Biochemistry.* **27,** 8063–8068
26. Pace, C. N. (1986) *Methods Enzymol.* **131,** 266–280
27. Clarke, J., and Fersht, A. R. (1993) *Biochemistry* **32,** 4322–4329
28. Kellis, J. T. J., Nyberg, K., and Fersht, A. R. (1989) *Biochemistry* **28,** 4914–4922
29. Otwinowski, Z., and Minor, W. (1997) *Methods Enzymol.* **276,** 307–326
30. McCoy, A. J., Grosse-Kunstleve, R. W., Storoni, L. C., and Read, R. J. (2005) *Acta Crystallogr. D. Biol. Crystallogr.* **61,** 458–464
31. Storoni, L. C., McCoy, A. J., and Read, R. J. (2004) *Acta Crystallogr. D. Biol. Crystallogr.* **60,** 432–438
32. Desmyter, A., Transue, T. R., Ghahroudi, M. A., Thi, M. H., Poortmans, F., Hamers, R., Muyldermans, S., and Wyns, L. (1996) *Nat. Struct. Biol.* **3,** 803–811
33. Brunger, A. T., Adams, P. D., Clore, G. M., DeLano, W. L., Gros, P., Grosse-Kunstleve, R. W., Jiang, J. S., Kuszewski, J., Nilges, M., Pannu, N. S., Read, R. J., Rice, L. M., Simonson, T., and Warren, G. L. (1998) *Acta Crystallogr. D. Biol. Crystallogr.* **54,** 905–921
34. Roussel, A., and Cambillau, C. (1989) *Silicon Graphic Geometry Partners' Directory,* pp. 71–78, Silicon Graphics, Mountain View, CA, pp. 71–78
35. Dumoulin, M., Last, A. M., Desmyter, A., Decanniere, K., Canet, D., Larsson, G., Spencer, A., Archer, D. B., Sasse, J., Muyldermans, S., Wyns, L., Redfield, C., Matagne, A., Robinson, C. V., and Dobson, C. M. (2003) *Nature* **424,** 783–788
36. Barthelemy, P. A., Raab, H., Appleton, B. A., Bond, C. J., Wu, P., Wiesmann, C., and Sidhu, S. S. (2008) *J. Biol. Chem.* **283,** 3639–3654

37. Aires da Silva, F., Santa-Marta, M., Freitas-Vieira, A., Mascarenhas, P., Barahona, I., Moniz-Pereira, J., Gabuzda, D., and Goncalves, J. (2004) *J. Mol. Biol.* **340,** 525–542
38. Myers, J. K., Pace, C. N., and Scholtz, J. M. (1995) *Protein Sci.* **4,** 2138–2148
39. Decanniere, K., Transue, T. R., Desmyter, A., Maes, D., Muyldermans, S., and Wyns, L. (2001) *J. Mol. Biol.* **313,** 473–478
40. Muyldermans, S., Cambillau, C., and Wyns, L. (2001) *Trends. Biochem. Sci.* **26,** 230–235
41. Tomlinson, I. M., Walter, G., Marks, J. D., Llewelyn, M. B., and Winter, G. (1992) *J. Mol. Biol.* **227,** 776–798
42. Griffiths, A. D., Williams, S. C., Hartley, O., Tomlinson, I. M., Waterhouse, P., Crosby, W. L., Kontermann, R. E., Jones, P. T., Low, N. M., and Allison, T. J. (1994) *EMBO J.* **13,** 3245–3260
43. Padlan, E. A. (1991) *Mol. Immunol.* **28,** 489–498
44. Roguska, M. A., Pedersen, J. T., Keddy, C. A., Henry, A. H., Searle, S. J., Lambert, J. M., Goldmacher, V. S., Blattler, W. A., Rees, A. R., and Guild, B. C. (1994) *Proc. Natl. Acad. Sci. U. S. A.* **91,** 969–973
45. Jespers, L., Schon, O., James, L. C., Veprintsev, D., and Winter, G. (2004) *J. Mol. Biol.* **337,** 893–903
46. Ward, E. S., Gussow, D., Griffiths, A. D., Jones, P. T., and Winter, G. (1989) *Nature* **341,** 544–546
47. Davies, J., and Riechmann, L. (1996) *Protein Eng.* **9,** 531–537
48. Tanha, J., Xu, P., Chen, Z., Ni, F., Kaplan, H., Narang, S. A., and MacKenzie, C. R. (2001) *J. Biol. Chem.* **276,** 24774–24780
49. Martin, F., Volpari, C., Steinkuhler, C., Dimasi, N., Brunetti, M., Biasiol, G., Altamura, S., Cortese, R., De Francesco, R., and Sollazzo, M. (1997) *Protein Eng.* **10,** 607–614
50. Riechmann, L. (1996) *J. Mol. Biol.* **259,** 957–969
51. Voordijk, S., Hansson, T., Hilvert, D., and van Gunsteren, W. F. (2000) *J. Mol. Biol.* **300,** 963–973
52. Decanniere, K., Desmyter, A., Lauwereys, M., Ghahroudi, M. A., Muyldermans, S., and Wyns, L. (1999) *Structure* **7,** 361–370
53. De Genst, E., Silence, K., Decanniere, K., Conrath, K., Loris, R., Kinne, J., Muyldermans, S., and Wyns, L. (2006) *Proc. Natl. Acad. Sci. U. S. A.* **103,** 4586–4591
54. Spinelli, S., Frenken, L., Bourgeois, D., de Ron, L., Bos, W., Verrips, T., Anguille, C., Cambillau, C., and Tegoni, M. (1996) *Nat. Struct. Biol.* **3,** 752–757
55. Tanha, J., Dubuc, G., Hirama, T., Narang, S. A., and MacKenzie, C. R. (2002) *J. Immunol. Methods* **263,** 97–109
56. Huang, S. C., Jiang, R., Glas, A. M., and Milner, E. C. (1996) *Mol. Immunol.* **33,** 553–560
57. Ohlin, M., and Borrebaeck, C. A. (1996) *Mol. Immunol.* **33,** 583–592
58. Jung, S., Spinelli, S., Schimmele, B., Honegger, A., Pugliese, L., Cambillau, C., and Pluckthun, A. (2001) *J. Mol. Biol.* **309,** 701–716